Analysis and experimental demonstration of temperature step gradients in preparative liquid chromatography

Xinghai An[a,*], Adnan Hayat[a], Ju Weon Lee[b],

Shamsul Qamar[c], Gerald Warnecke[b], Andreas Seidel-Morgenstrern[a,b]

[a] Max Planck Institute for Dynamics of Complex Technical Systems, Sandtorstraße 1, 39106 Magdeburg, Germany
[b] Otto von Guericke University Magdeburg, Universitätsplatz 2, 39106 Magdeburg, Germany
[c] COMSATS University Islamabad, Islamabad 45550, Pakistan
[*] Corresponding author: an@mpi-magdeburg.mpg.de

Abstract

The amount of substance adsorbed on solid surface depends on temperature. Therefore, the migration velocities of the solutes in a chromatographic column can be altered by introducing temperature gradients. Such gradients designed to change retention behaviours can be exploited to improve the separation performances in preparative chromatography. To describe key process features, we used analytical solutions of the equilibrium model with instant stepwise shift of temperature. To achieve a more realistic description, the equilibrium dispersion model was additionally applied to treat finite column efficiencies. The effect of temperature gradients was illustrated experimentally using two identical columns sequentially connected. Temperature of the second column was modulated by thermostats. Wide pulse injections of a single component led to instructive elution profiles in a preliminary investigation. The observations were found to be in qualitative agreement with predictions of the equilibrium dispersion model. Subsequently, the separation of a ternary model mixture was investigated considering a simple two-step temperature gradient. To support the quantitative analysis and to identify suitable switching and cycle times, the temperature dependencies of the Henry constants were determined by short pulse injections. A meaningful variation of the parameters of the temperature gradient is required for adjusting the cycle times, which is the time difference between two consecutive injections that needs to shorten. Decreasing this time is connected with a desirable increase in process productivity. The results achieved revealed that relatively simple to implement stepwise temperature gradients offer an option to improve and fine-tune the performance of repetitive batch chromatography.

Keywords: Batch chromatography; linear isotherms; temperature gradients; cycle times; productivity

1. Introduction

Chromatography is a widely applied separation technology, for example in the pharmaceutical, petrochemical, and biochemical industries. Substantial research activities have been carried out to improve the performance of preparative chromatographic processes by developing new degrees of freedom that allow increasing productivities and purities [1,2]. Significant progress was attributed to the development of multi-column simulated moving bed chromatography, which applies a virtual counter current between the solid and liquid phases [3,4]. However, this sophisticated process is applicable accompanied by significant capital and operating costs. The application of gradient operation in a single column offers a simpler alternative. The widely applied concept is based on the periodic modulation of certain operating parameters during the chromatographic separation process. These modulations (gradients) can locally and temporarily alter the strength of the solute-solid interactions and thus manipulate the migration velocities of the components. It is well known that the course of the adsorption isotherms as a measure of binding strength can be influenced by numerous parameters as for example the type of adsorbent, the type of solvent, the pH value, pressure, and temperature. Accordingly, there are widespread theoretical and experimental investigations as well as applications regarding solvent gradients [5–8], adsorbent type gradients [9,10], pH gradients (particular in bioseparation [11–13]), pressure gradients [14] and numerous more including temperature gradients. The latter are frequently applied in gas chromatography, changing the temperature of the whole column ([5][15,16]). In this field it is relevant that temperature can alter the fluid phase viscosity and might influence the pressure. Potential applications of temperature gradients in preparative chromatography are seen in performing separation with components in the elution train that travel significantly faster or slower than the majority, sometimes called “partly lagged separations”, which might benefit from a temperature tuning close to the column end. A possible key advantage compared to isocratic (isothermal) separation is the potential to reduce the cycle time, i.e. the time difference between consecutive injections. This can be achieved by deceleration of the fast migrating components and/or acceleration of the slow migrating components. Furthermore, in case of coelution of components purity benefits can be achieved from temperature

gradients by increasing the resolution. Another advantage compared to the application of solvent gradients is the avoidance of a more complicated solvent handling.

Temperature gradients can be classified according to the way the temperature modulation is introduced. A so-called inlet modulation can be performed by changing the temperatures of the fluid (solvent or sample) introduced at the column inlet. Regarding the usage of deviating temperatures of the samples injected the terms “hot” or “cold” injections are used [17,18]. Many studies have been carried out to examine the temperature effect on chromatographic separations in single columns [19] and multi-column simulated moving bed processes [20–22]. In contrast to creating gradients with the temperature of the fluids entering the columns, an alternative external temperature modulation can be performed by applying several jackets around the column wall for segmented heating or cooling with suitable external fluids, e.g. water. This type of external heating or cooling can be also realized using electrical heating bandages [23,24]. It was reported in [25] that in case of a simulated moving bed process a temperature modulation triggered through establishing a temperature difference over the column wall performed better than an internal modulation using temperatures changes related to the feed and solvent streams. As the more frequently applied gradients in the solvent composition, temperature gradients can also be classified according to the functional dependence of the parameter modulated on time and/or column position. Simple cases are temperature step gradients and linear temperature gradients.

Theoretical results regarding the overall retention behaviour subjected to temperature gradients over space are available [26]. It is also possible to impose temperature changes over time which are active on the entire column as described in [27–29]. Obviously, the most promising option is to modulate the temperature both over the space coordinate and the time coordinate, respectively. This flexible approach was described to be very attractive for solving separation tasks [30,31].

We describe below a theoretical and experimental analysis of externally modulated temperature step gradients. In a simulation study, the one-dimensional model neglecting radial gradients can be used [32]. To approximate this, the columns should be slim and should offer a large surface to volume ratio. If possible, adsorbent particles with high thermal conductivity should be applied. To decrease process complexity, simple segmentation scenarios are preferable.

Below we will consider exclusively temperature profiles, which are just two-step functions over both the column length coordinates and time. With respect to the length coordinate we will illustrate essential effects of temperature changes for a column, which is divided into two segments with equal length. The temperature is periodically altered in a stepwise manner only in the second segment exploiting three levels. The switch times, t_s, need to be adjusted according to the specific separation problem. Obviously, further improvements could be achieved by implementing more column segments and applying more sophisticated temporal temperature profiles. However, we will not address such extensions in this paper.

Using the classical equilibrium model (EM)[33] we derived analytical solutions in our previous theoretical work assuming perfect temperature step gradients [34]. These instructive solutions describe the most optimistic scenario and provide an instructive insight into the effect of temperature gradients. Below we will present in addition also another still quite simple but already more realistic model, namely the equilibrium dispersion model (EDM). The corresponding model equations of the EDM can be solved only numerically. Both models allow estimating cycle times and, thus, productivities of a periodic regime exploiting repetitive batch injections.

The first part of the experimental section of this paper will provide an illustration of the effect of temperature gradients on the elution behaviour of single rectangular injections of ternary model mixture. For these investigations two identical columns were connected in series via a short and thin capillary, which allowed to consider them as a single column. The temperature in the first column segment was kept permanently at a reference temperature T_R. To introduce step gradients the temperature in the second column segment could be set at a certain switch time t_s to a, compared to T_R, higher (T_H) or lower temperature (T_L).

We will then present the results of preliminary measurements performed to estimate for the three components of the selected ternary model mixture the essential thermodynamic and kinetic parameters of the EM and the EDM.

Subsequently, we will illustrate the impact of different types of temperature gradients on experimentally determined courses of single component wide pulse injections and a comparison of the observations with model predictions.

Finally, we will analyse repetitive injections of mixtures of the three components. To discuss the relevance of minimising the cycle times, i.e. the time differences between consecutive injections, we will present predictions of the EM model and EDM model and corresponding experimentally determined chromatograms. It will be shown, how a) to estimate an upper limit of the productivity gain achievable using such temperature gradient concepts and b) to identify suitable times for switching the temperatures. A strategy will be described how to estimate safety margins for the cycles times, which are needed to compensate deficits of EDM prediction based on assuming ideal temperature gradients.

2. Theoretical background

2.1 Equilibrium model (EM) assuming instant temperature shift

In our previous study [34], the well-established 1-D equilibrium model of chromatography [33] was extended to describe ideal temperature step gradients. The model consists of the basic mass balances of all components *i* of an *N*-component mixture:

$$\left(1 + \frac{1-\epsilon}{\epsilon}\frac{dq_i}{dc_i}\right)\frac{\partial c_i}{\partial t} + u\frac{\partial c_i}{\partial z} = 0 \qquad i = 1, N \tag{1}$$

where t and z respectively represent time and space variables, q_i and c_i are respectively the stationary and mobile phase concentrations, u is the interstitial velocity, and ϵ_T is the total porosity defined as:

$$\epsilon_T = \frac{4\dot{V}(t_0 - t_d)}{\pi L D_c^2} \tag{2}$$

where L and D_c respectively represent the length and the diameter of column, $\dot{V}$ is the volumetric flow rate and t_0 and t_d are the tracer retention and the system dead times, respectively.

As in our previous theoretical study [34], we assume below linear adsorption isotherms:

$$q_i = a_i(T)c_i \qquad i = 1, N \tag{3}$$

To justify the application of Eq. (3), the experiments described below were carried out under diluted conditions. To describe the temperature dependency of the Henry constants $a_i(T)$, the Van't Hoff relation can be used:

$$a_i(T) = \left.\frac{dq_i}{dc_i}\right|_T = a_{i,R}(T_R)exp\left[\frac{-\Delta H_{A,i}}{R}\left(\frac{1}{T} - \frac{1}{T_R}\right)\right] \qquad i = 1, N \tag{4}$$

where T_R represents a reference temperature, $a_{i,R}$ the Henry constant at this temperature, $\Delta H_{A,i}$ the adsorption enthalpy for component i and R the universal gas constant. The Henry constants can be determined for a given temperature T from:

$$a_i(T) = \frac{\epsilon_T}{1-\epsilon_T}\left(\frac{t_{R,i}(T)-t_d}{t_0-t_d} - 1\right) \qquad i = 1, N \tag{5}$$

where $t_{R,i}$(T) represents the experimentally accessible retention time of species i at a given temperature T.

The inlet boundary conditions for the first column segment required to solve Eq. (1) are for N_{inj} periodically repeated identical injections over a time Δt_{inj} for an injection concentration $c_{f,i}$:

$$c_{i,segment\ 1}(t, z = 0) = \begin{cases} c_{f,i} & t \in \left[\, t_{inj}^{k}, t_{inj}^{k} + \Delta t_{inj}\right] \\ 0 & t \in \left[t_{inj}^{k} + \Delta t_{inj}, t_{inj}^{k+1},\right] \end{cases} \quad i = 1, N;\ k = I, II, \ldots \tag{6}$$

where t_{inj}^{k} marks the start time of the k^{th} injection in roman numeral. Note that the injection profile is assumed to be of ideal rectangular shape. Unavoidable non-idealities can be lumped into the apparent dispersion coefficient.

The inlet boundary conditions for the second column segment are:

$$c_{i,segment\ 2}(t, z = 0) = c_{i,segment\ 1}(t, z = z_{switch}) \qquad i = 1, N \tag{7}$$

where z_{switch} indicates switching position. In this study, we exclusively used $z_{switch}=0.5L$, though other splits could be treated analogously. The temporal and axial temperature profile $T(t,z)$ are prescribed exploiting just three temperature values, namely T_R, T_H or T_L. For the whole first segment of the column a reference temperature is assumed:

$$T_{segment\ 1}(t, 0 < z <= z_{switch}) = T_R \tag{8}$$

Also in the whole second segment of the column there is at any time a constant value for the temperature assumed:

$$T_{segment\ 2}(t, 0 < z <= z_{switch}) = T^*(t) \quad with\, T^*(t) \in [T_R, T_H, T_L] \tag{9}$$

In the gradient case the value for $T^*(t)$ changes periodically in a hypothetical perfect step-wise manner between the three levels (T_R, T_L, T_H) changed at characteristic switch times t_s. The specification of this temporal switch regime defines the temperature gradient shape. In case of implementing a repetitive injection regime several switch events can be performed in the period of eluting a certain injected amount.

In Fig. 1 we illustrate essential features of the described single-step temperature gradients by presenting selected results for a single solute injection. We used selected analytical solutions of the EM based on [34]. Keeping the injection times and concentrations constant, three different scenarios are compared in which the temperature courses imposed to the second segment were different. Space-time diagrams illustrate the characteristic pathways of the traveling adsorption and desorption fronts. For linear isotherms these pathways are straight lines and the slopes correspond to the component specific migration velocities that is altered by temperature, cf. Eq. (4)-(5) [33,34].

In Fig. 1 three sub-plots are given for three different switch times used in the second column. For these three switch times both cases are shown, namely a step to a higher temperature, T_H (red curves), and a step to a lower temperature, T_L (blue curves). In addition, the isothermal (isocratic) case is also shown at T_R (green curves).

Fig. 1(a) shows the band characteristics for the case that the switch at t_s=0 is immediately activated. Thus, the migration velocities of the adsorption and desorption fronts immediately change when they reach to the second segment. This effect is equivalent when the effective temperature gradient starts before the adsorption front has reached the second segment and after the desorption front has left from the second segment (dark grey zone for the case of T_R). In the figure are further illustrated the widths of the bands, w, and the local distributions between the two phases in the second segment at different characteristic times t^* (marked as colour dots). With respect to elution at the column outlet, the same concentration profiles are predicted by the EM for all three scenarios.

In Fig. 1(b) a scenario that the temperature switch is imposed when the desorption front reaches the inlet of the second segment. This means that the complete sample enters the second segment under the isothermal conditions. The occurrence of the simultaneous migration velocity changes of both adsorption and desorption fronts maintains the same band width over the space coordinate w_z but leads to a compressed or broadened outlet elution profile for T_H or T_L, respectively. Consequently, the outlet concentrations are different.

As the final example Fig. 1(c) depicts a situation in which a temperature switch is imposed when already a part of solute has left the second segment under the isothermal conditions. In this case, the part of the solute that is still inside the column is affected by the gradient. Such

late interfering gradients create elution profiles are characterized by two distinct concentration levels. In case of increasing the temperature an eventually attractive situation arises characterized by narrower bands connected with higher concentration.

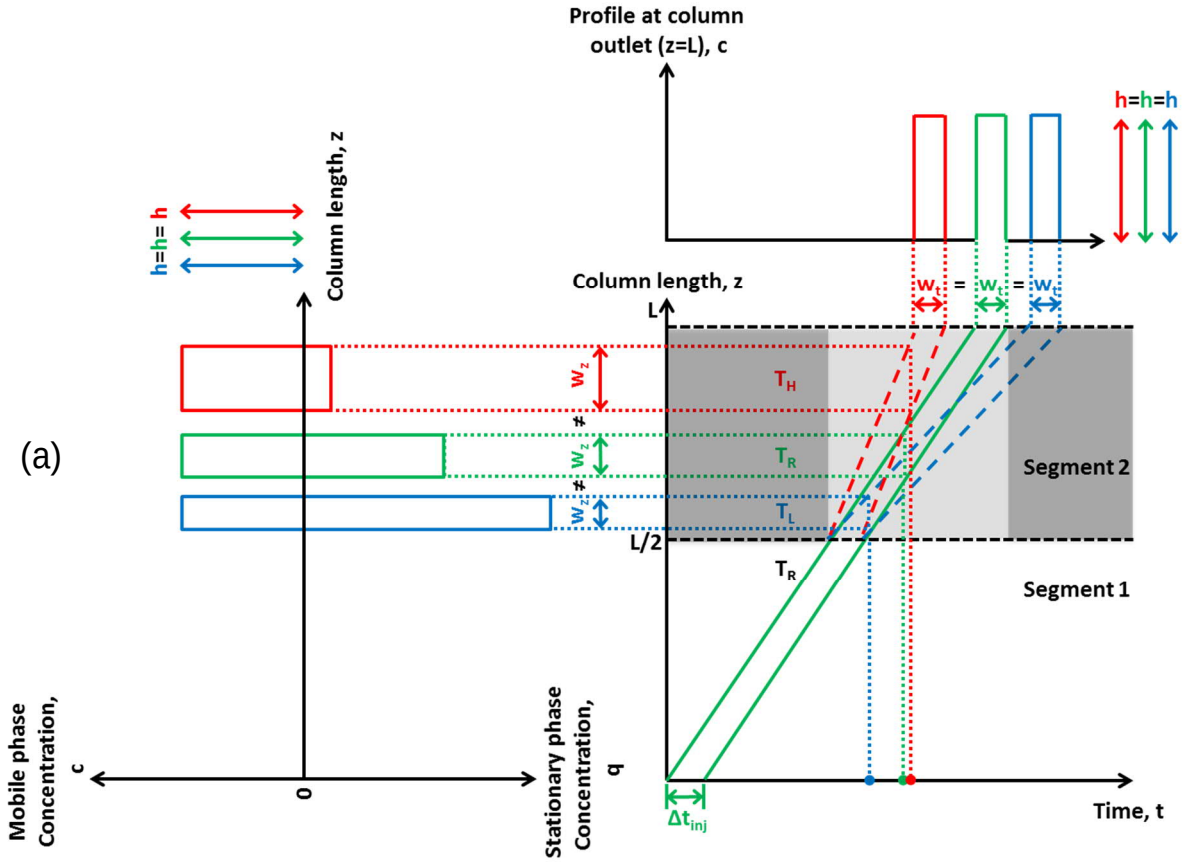

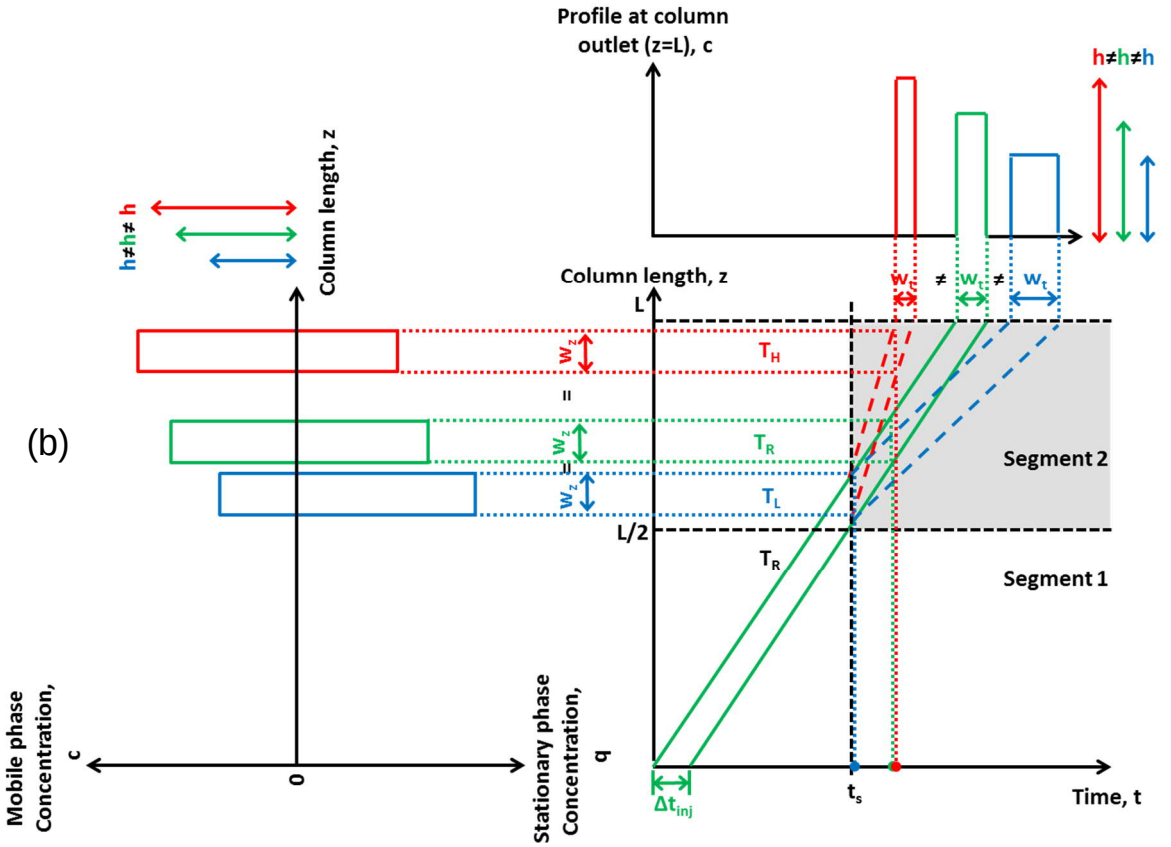
(b)
Profile at column outlet (z=L), c
h≠h≠h
Column length, z
h≠h≠h
Column length, z
L
L/2
0
w_z
T_H
T_R
T_L
Segment 2
Segment 1
Mobile phase Concentration, c
Stationary phase Concentration, q
Δt_{inj}
t_s
Time, t

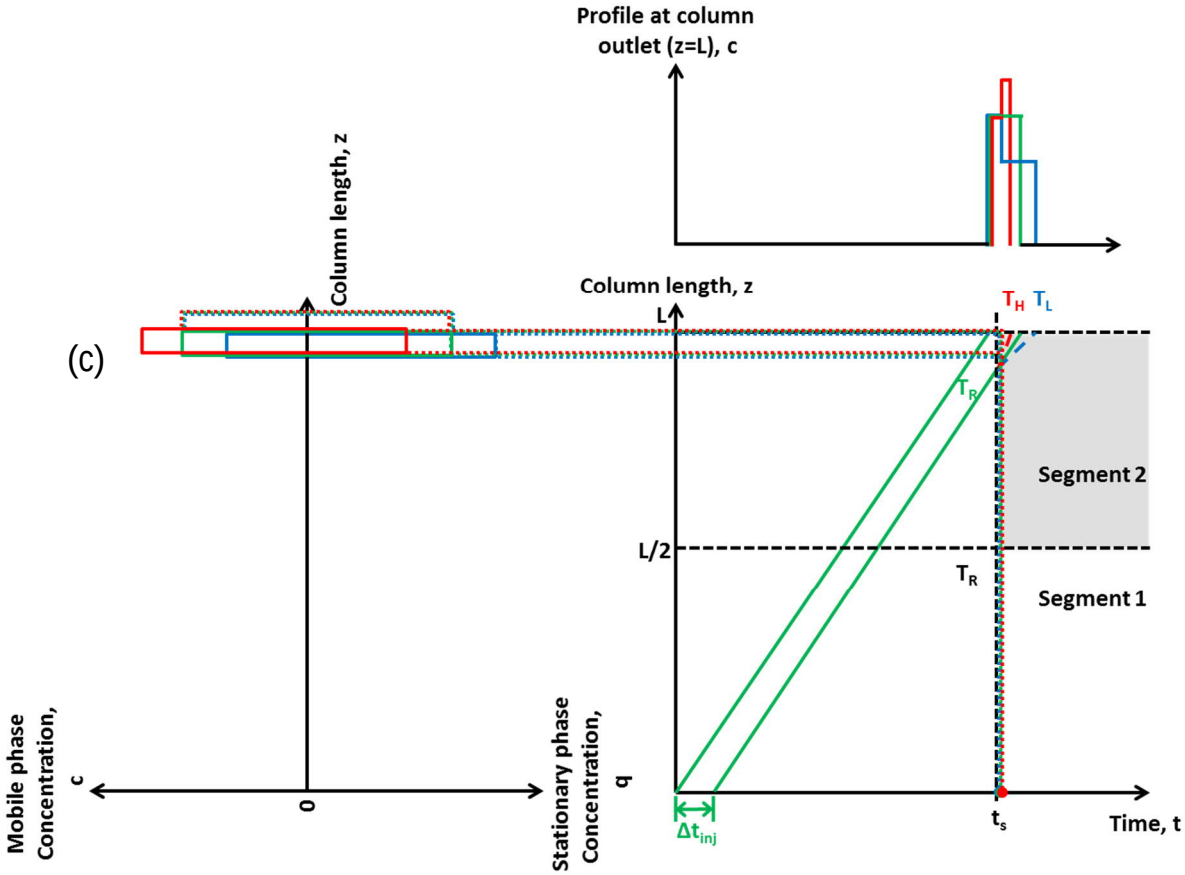
(c)
Profile at column outlet (z=L), c
Column length, z
Column length, z
L
L/2
0
T_H T_L
T_R
Segment 2
Segment 1
Mobile phase Concentration, c
Stationary phase Concentration, q
Δt_{inj}
t_s
Time, t

Fig. 1. Illustration of the effect of different types of step-gradients using space-time trajectories as predicted by the EM. Green solid lines represent isothermal operation at reference temperature T_R. The red and blue dashed lines represent scenarios where heating (T_H) and cooling (T_L) of the second segment was performed at specific switch times, t_s. Shown are three different scenarios belong to three different switch times (top: t_s=0; middle: t_s when desorption branch reaches second segment, bottom: t_s when a part of the solute has already left the second segment). The plots are complemented by illustrating the corresponding chromatograms at the column outlet, *c(t,z=L)*, and the local fluid and solid phase concentrations at three characteristic times t^*, *c(t^*,z)* and *q(t^*,z)*. Here, h indicates the band concentration heights and w_t and w_z indicate band widths over time and space, respectively. The grey marked blocks indicate the modulation of temperature levels.

2.2 Equilibrium-dispersion model assuming ideal temperature steps (EDM)

A straightforward extension of the simple EM described and exploited above is the equilibrium-dispersion model (EDM). We used this model in this work again combined with the simplifying assumption of ideal temperature steps. The EDM differs from the EM (Eq. (1)) just by introducing a second order axial dispersion term [1,2]:

$$\left(1 + F\frac{dq_i}{dc_i}\right)\frac{\partial c_i}{\partial t} + u\frac{\partial c_i}{\partial z} = D_{app,i}\frac{\partial^2 c_i}{\partial z^2} \qquad i = 1,N \tag{10}$$

The apparent axial dispersion coefficient D_{app} describes lumped deviations from infinite column efficiency [1]. It can be well-estimated by exploiting the number of theoretical plates N_p, which can be determined by analysing classical pulse experiments [1]:

$$D_{app,i} = \frac{Lu}{2N_{p,i}} \qquad i = 1,N \tag{11}$$

For symmetrical peaks observed in the linear isotherm range, N_p can be conveniently estimated by

$$N_{p,i} = 5.54\left(\frac{t_{R,i}}{w_{0.5,i}}\right)^2 \qquad i = 1,N \tag{12}$$

where $t_{R,i}$ indicates the retention time and $w_{0.5,i}$ is the width at half height of the response to a pulse injection of component *i* [1,2]. The usage of Eq. 12 to estimate Np also evaluates the impact of both non-ideal inlet profiles and the already starting peak distortion due to modest column overloading. Thus, the intrinsic column efficiency would be higher, i.e. the corresponding "ideal" dispersion coefficient would be lower. For the purpose of our study the

overestimation of this coefficient is helpful and intended, since it represents a lumped parameter that captures all band broadening effects.

Solving the EDM equations needs the provision of a second boundary condition. Typically and also in our work the following outlet condition is used:

$$\frac{\partial c_i}{\partial z}(t, z = L) = 0 \qquad i = 1, N \tag{13}$$

The mass balance equations of the EDM can be solved only numerically. We applied a finite volume scheme with upwinding for the advection term based on [35].

2.3. Performance criteria to evaluate periodic repetitive injections

A commonly used criterion for the evaluation of the performance of chromatographic separation processes is the following productivity P_i:

$$P_i = \frac{m_{o,i}}{V_C(\Delta t_{cyc} + \Delta t_{safe}^T)} \qquad i = 1, N \tag{14}$$

where $m_{o,i}$ represent the mass collected during one cycle, V_C is column volume. Δt_{safe}^T is the safety time for non-ideal implementation of the temperature gradient, which is unavoidable in certain cases. The cycle time Δt_{cyc} is defined in a repetitive k^{th} cycle:

$$\Delta t_{cyc} = t_{N,end}^k\Big|_{c_{thres}} - t_{1,start}^k\Big|_{c_{thres}} \tag{15}$$

To avoid remixing within the column, this cycle time can be calculated by the time difference between the end point of the last eluting component and the start point of the first eluting component. The cycle times were determined in the different design steps using the EM and EDM as well as in the experimental validations (EXP). To identify these characteristic times, problem specific concentration or detector signal can be used as threshold values c_{thres}.

The larger cycle time predicted by the EDM can be estimated from the corresponding cycle time of the EM by adding a safety margin Δt_{safe}^{Mod}.

$$\Delta t_{cyc}(EDM) = \Delta t_{cyc}(EM) + \Delta t_{safe}^{\mathrm{Mod}} \tag{16}$$

3. Materials and Methods

In the current study, cyclopentanon (C5), cyclohexanon (C6) and cycloheptanon (C7) purchased from Alfa Aesar were used as solutes. A C18 column (Agilent Zorbax Eclipse XDB, D_c=4.6 mm, L=100 mm, particle size=5 µm) was used as stationary phase whereas Methanol from Sigma-Aldrich and distilled water filtrated with 0.45 µm filter paper from Sartorius Stedim Biotech GmbH (50%/50%, v/v) were used as mobile phase. Under these reverse phase conditions the corresponding peaks appear in the order C5, C6 and C7. The injection concentrations $C_{f,i}$ used in this work were 0.1 vol% corresponding to 0.949 g/L, 0.948 g/L and 0.956 g/L, respectively. The concentrations considered were experimentally confirmed in preliminary experiments to be in the linear isotherm range by confirming that the key features of the elution profiles do not change with varying the injection volume. Volumes in the range of 50-1500 µL were introduced using both syringe and pump injections. The column porosity ϵ_T was estimated using Thiourea (Merck) as tracer. Marker experiments were performed to estimate extra-column dead times. Taking pressure drop, acceptable residence times and heat exchange into account, the flow rate $\dot{V}$ was fixed for all experiments at 0.3 ml/min.

The experimental system of segmented temperature gradient liquid chromatography is illustrated in the Fig. 2. The system consists of a classical HPLC set (Hewlett Packard 1100) and an extended temperature modulating unit with insulation. The wavelength of the detector in the current work was fixed as 280.2 nm. The detector calibration factors of C5, C6, C7 were determined to be 0.004, 0.005 and 0.005 $gL^{-1}mAU^{-1}$, respectively. Two columns are connected in series to form the segment gradient. The first column (Segment 1) is placed in the HPLC oven and the temperature is kept at reference temperature ($T_{Segment\ 1}=T_R$=25 °C) and the second column (Segment 2) is placed in a cylindrical water jacket. The temperature of Segment 2 is manipulated stepwise by the externally circulating water from two thermostats to low temperature T_L or high temperature T_H. Thermostats can internally or externally circulate water by four three-way switch valves. Before each switch, the cold water flows externally through the water jacket in counter-current manner while the hot water flows internally in the thermostats, and vice versa. Upon switching valves, the water in the water jacket can be replaced by that from the other thermostat with different temperature. The temperatures in the water jacket T^A and at the column outlet T^B were measured by two thermocouples. The temperature profiles presented in figures are water jacket temperatures, T^A. Due to the technical difficulty in measuring the actual internal temperature of the column $T_{Segment\ 2}$ or capillary outlet, the temperature on the outer surface of outlet was instead measured. Both

measured temperatures were recorded in real time. In this study, equilibrium between column interior, column wall and surrounding water from the thermostat was assumed, i.e., $T_{Segment\ 2}=T^*$. For the sake of safe operation range of the column, the temperature range was set from T^*=5-60 ˚C. The rate of heat transfer in the current work was found to be relatively fast to realise with good approximation the planned temperature gradients.

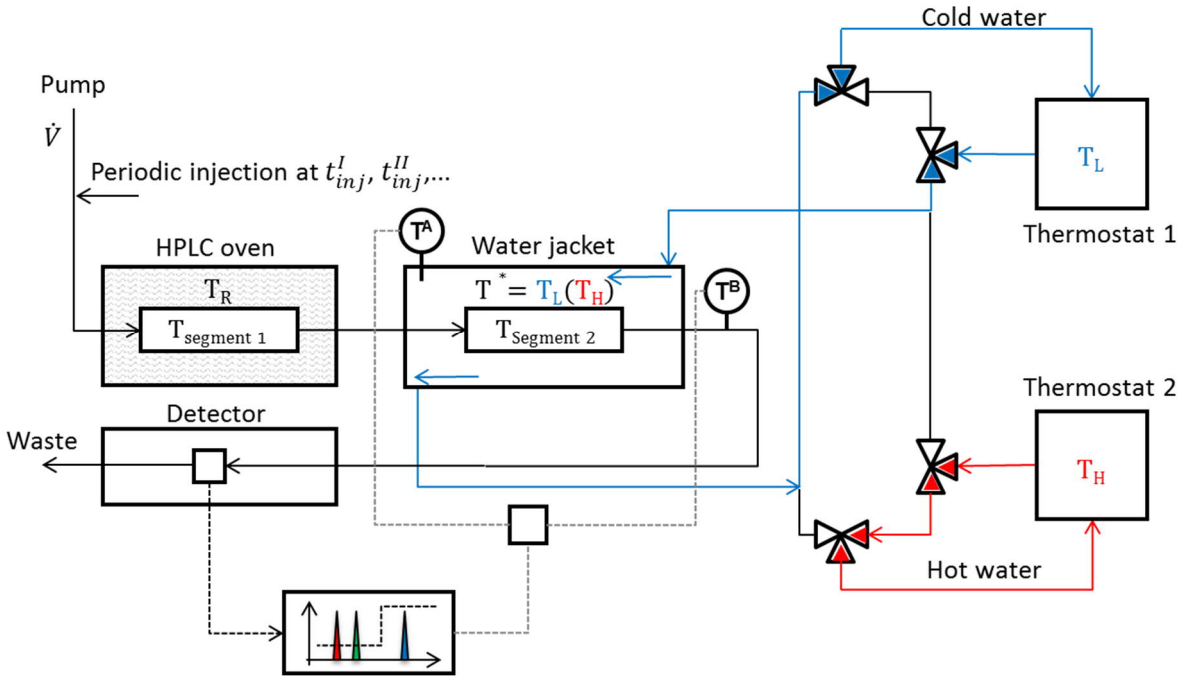

Fig. 2. Experimental system of forced segmented temperature gradient liquid chromatography. It is composed of HPLC unit, water jacket and thermostats. The flow rate from the pump was fixed at $\dot{V}$=0.3 ml/min. Two fluids inside and outside the water jacket flow in a counter-current manner. The temperature in the oven was kept as reference temperature, $T_R=T_{Segment\ 1}$=25°C. Two thermal couples are placed in the water jacket, $T_{Segment\ 2}=T^*=T_L$ or T_H. The real temperatures are measured for water T^A and the outer surface of the outlet line T^B.

4. Results and discussions

4.1 Illustration of the impact of temperature step gradient

A typical chromatogram recorded under isothermal conditions at T_R=25°C was shown in Fig. 3. From this chromatogram a cycle time Δt_{cyc}=12.7 min can be estimated assuming both the first and the last eluting components a threshold signal of 5 mAU. There is a significant gap

between the C6 and C7 peaks. It can be reduced for example by using solvent gradients. However as shown in Fig. 3(b) it can be also achieved by imposing a single-step temperature gradient, which can reduce cycle time Δt_{cyc}=11.4 min while maintaining resolution for the selected gradient.

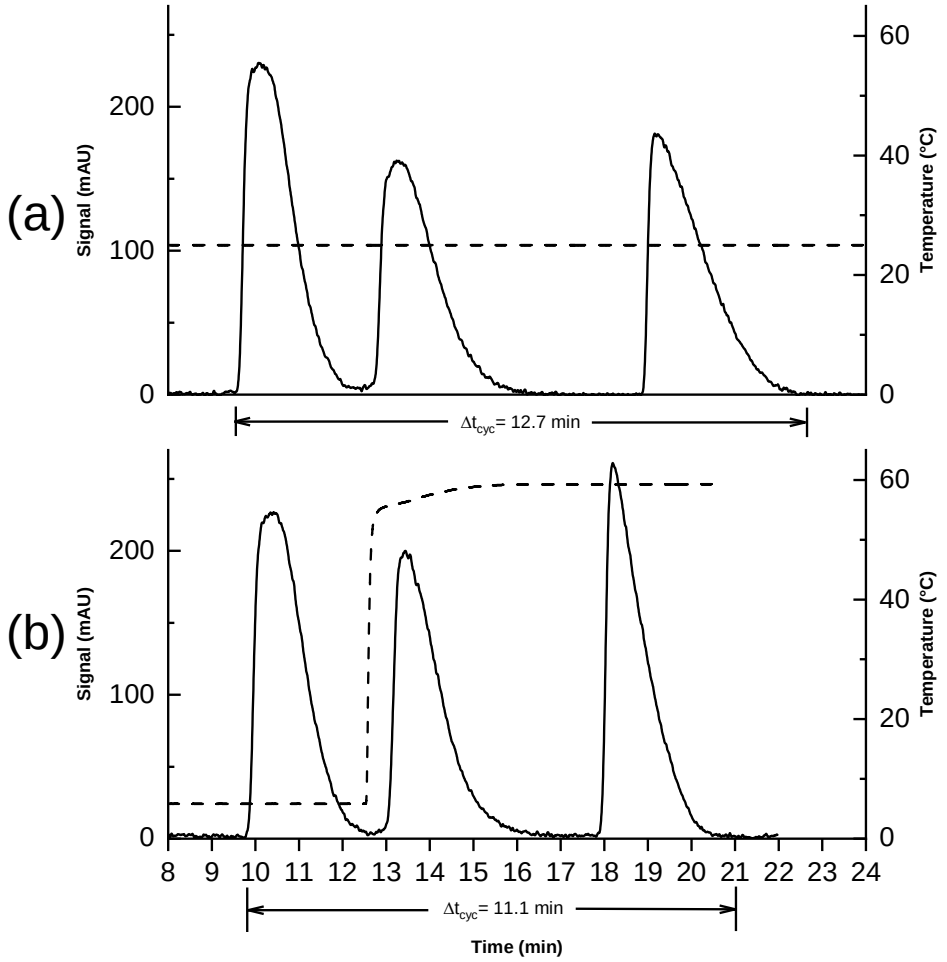

Fig. 3. Comparison of single injection of a ternary mixture under isothermal and gradient operations. Solid line corresponds to chromatogram (left axis) and dash line to temperature (right axis). (a) Isothermal operation at 25 °C, Δt_{cyc}=12.7 min. (b) Gradient operation. T_L=5°C, T_H=60°C, Δt_{cyc}=11.4 min. $c_{f,C5}$=0.949 g/L, $c_{f,C6}$=0.948 g/L, $c_{f,C7}$=0.956g/L, $V_{inj}=\dot{V}\Delta t_{inj}$=400 µL, $\dot{V}$=0.3 ml/min. The cycle time Δt_{cyc} is calculated by Eq. (15).

4.2 Estimation of thermodynamic and kinetic parameters required in the EM and EDM

As aforementioned, taking pressure drop, acceptable residence times, and heat exchange into account, the flow rate $\dot{V}$ was fixed for all experiments at 0.3 ml/min. First, the system dead time t_d was determined to be 0.25 min by injecting small amount of tracer without column installed. After that, the tracer retention time t_0 was determined to be 3.075 min by injecting

small amount of tracer with column installed. Thus the column porosity ε_T was calculated to be 0.555 by Eq. (2).

Then the initial isotherm slopes were determined for each of the three components within a broader temperature range. Retention time $t_{R,i}$ of each component at each temperature with injection volume of 50 µL can be obtained to calculate the Henry constant a_i by Eq. (5). The Henry constants according to component and temperature as well as heats of adsorption are summarised in Table 1. The Henry constant of one component had an oblivious difference compared to the rest of components, which leads to a partly lagged separation problem. If this distance is similar, then the applicability of temperature gradient can be limited. The van't Hoff plot of each component by linearising Eq. (4) is illustrated in Fig. 4. It can be observed that $\ln(a_i/a_{i,R})$ was not perfectly linearly related to 1/T. In the temperature range between 10 and 40°C, they were correlated in a linear manner, however, a polynomial behaviour was found beyond this range, which manifested a more complicated thermodynamics. If linear regression within the entire range was applied, the heat of adsorption $\Delta H_{A,i}$ of C5, C6 and C7, by taking the slopes from the plot, were calculated to be -5.481 kJ/mol, -6.674 kJ/mol and -8.180 kJ/mol, respectively. C7 was relatively more sensitive to temperature than C5 and C6 so that main influence of C7 on performance can be expected.

Finally, the theoretical plate number for all three components was calculated from Eq. (12) with the widths of pulse responses at the flow rate of 0.3 ml/min and the averaged $\overline{N_p}$ was determined to be 2871. Thus, the averaged apparent dispersion coefficient $\overline{D_{app}}$ was estimated to be 0.0057 cm^2/min from Eq. (11).

After these preliminary experiments all parameters were available which are required to use the EM and the EDM to predict chromatograms under temperature gradient conditions and to compare the results with experiments. All relevant parameters are summarised in Table 2. In addition, the system dead time in wide pulse experiments, see section 4.3, was determined to be 3.246min, whereas 0.25 min in other experiments. The operating conditions used in specific experiments are shown in Table 3. In mixture experiments, our goal is to develop a periodic temperature switching regime to reduce cycle time.

Table 1 Henry constants a_i of each component derived from mean retention time $t_{R,i}$ for different temperatures and heats of adsorption ΔH_A.

Temperature, T^A (°C)	Henry constants, a_i

(Fig. 2)	C5	C6	C7
5.80	0.781	1.572	3.186
10.65	0.769	1.518	3.061
15.50	0.736	1.453	2.894
20.40	0.717	1.401	2.768
25.26 (T_R)	0.693	1.343	2.630
30.18	0.670	1.285	2.485
35.04	0.647	1.231	2.361
39.91	0.626	1.181	2.251
44.80	0.603	1.140	2.141
49.68	0.578	1.084	2.014
54.57	0.558	1.033	1.911
59.39	0.536	0.988	1.808
Heat of adsorption (kJ/mol)	-5.481	-6.674	-8.180

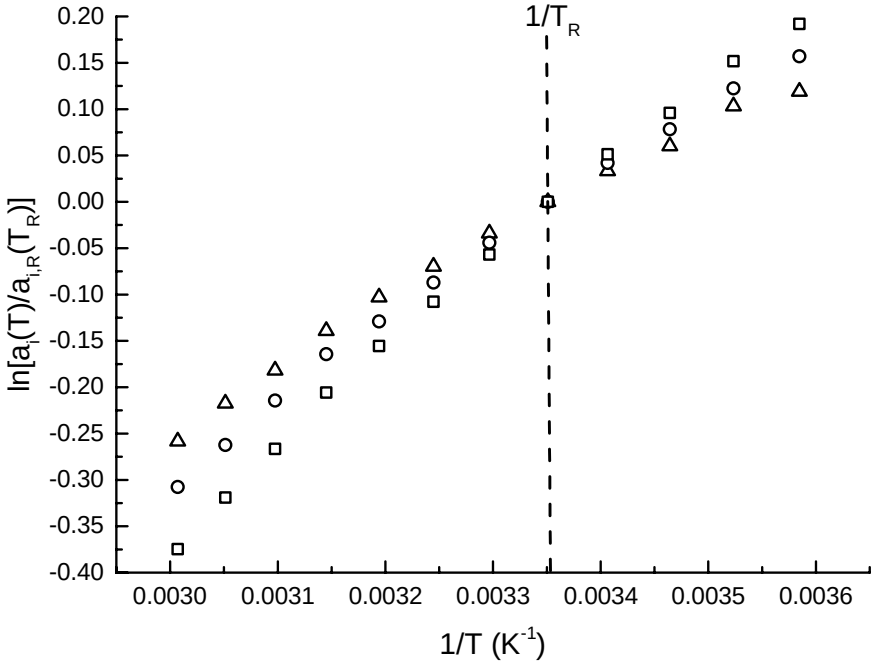

Fig. 4. Van't Hoff plot of each component: C5 (triangle), C6 (circle) and C7 (square). Data were calculated based on Table 1. $c_{f,C5}$=0.949 g/L, $c_{f,C6}$=0.948 g/L, $c_{f,C7}$=0.956g/L, V_{inj}=50 µL, $\dot{V}$=0.3 ml/min.

Table 2 Summary of common parameters used in simulation.

Symbol	Quantity	Value	Remark
L	Length of column	20 cm	
D_c	Diameter of column	0.46 cm	
$\dot{V}$	Flow rate	0.3 ml/min	
ε_T	Porosity of column	0.555	Eq. (2)
F	Phase ratio	0.802	
t_d	Dead time	0.25min*, 3.246 min**	

$c_{f,i}$	Injection concentrations of C5, C6 and C7	0.949, 0.948 and 0.956 g/L	0.1/0.1/0.1 vol%
$\overline{N_p}$	Theoretical plate number (average of all three components)	2871	Eq. (12)
$\overline{D_{app}}$	Averaged Apparent dispersion coefficient	0.0057 cm^2/min	Eq. (11)

* Section 4.2, Section 4.4
**Section 4.3

Table 3 Summary of operating conditions according to different experiments.

Symbol	Quantity	Parameter determination (Section 4.2)	Single component wide pulse injections (Section 4.3)	Mixture experiments (Section 4.4)
Δt_{inj}	Injection period	0.17 min	5 min	1.33 min
$V_{inj}=(\dot{V}\Delta t_{inj})$	Injection volume	50 µL	1500 µL	400 µL
T_L	Low temperature	5°C	10°C	5°C
T_H	High temperature	60°C	40°C	60°C

4.3 Effect of temperature gradients on elution behaviour of a single component

The retention behaviour of a single component in wide injection was both theoretically and experimentally investigated to illustrate the concept of temperature gradient in an intuitive manner. First of all, the dead time should be redetermined since the solvent tank was used as the component reservoir to generate plateaus. By injecting a small amount of sample without the column, the dead time from mixer to detector was found to be 3.246 min. In this experiment, C7 was injected since it has the biggest thermal sensitivity among the components. The injection lasted for 5 min, i.e., the injection volume was 1500 µL. The gradient operations according to the switch time mentioned in section 2.1 were performed.

4.3.1 Preliminary theoretical EM and EDM predictions for wide pulses

In order to examine the consistency of analytical solutions of the EM and the numerical solutions of the EDM, first theoretical calculations were performed considering the gradient described in Fig. 1(bottom). In Fig. 5 the distinct band splitting predicted by the EM is shown. In good agreement the profile the EDM predicts a split at the same position but is characterized by a more realistic dispersion. The significant effect of the theoretical plate number as the additional free parameter of the EDM is illustrated that the larger the plate number, the smaller the dispersion. For very large plate numbers, the numerical solution

approaches the analytical solution of the EM. The mass balance was checked and revealed an almost perfect agreement with the analytical solution.

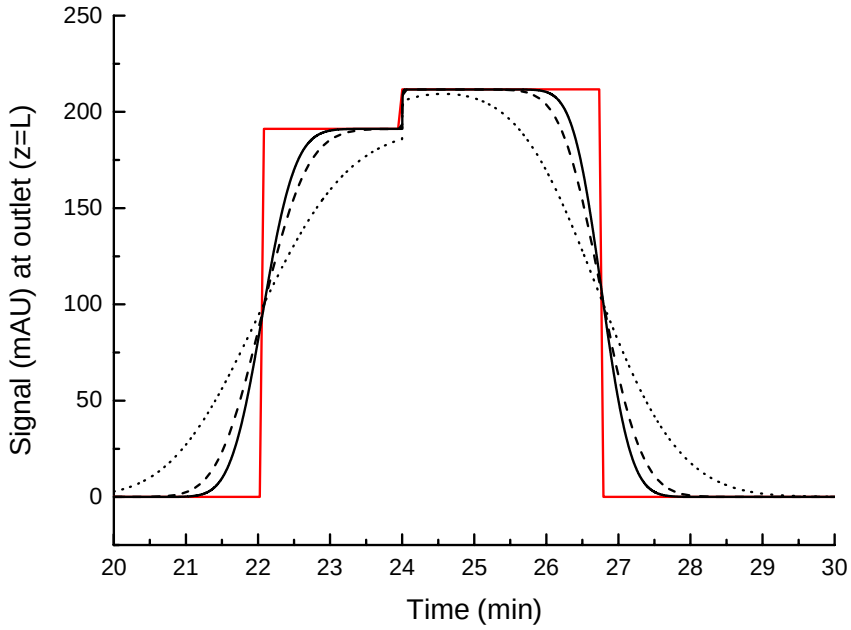

Fig. 5. Simulation of single component retention behaviour in wide pulse injection including dead time, corresponding to the red line in Fig. 1(c). Red solid line represents analytical solution using EM ($\overline{N_p} = \infty$) and black lines represent numerical solution using EDM with $\overline{N_p}$=200 (dotted), 1000 (dashed) and 2871 (solid). $c_{f,C7}$ =0.956 g/L, t_{inj}=0 min, V_{inj}=1500 µL, $\dot{V}$=0.3 ml/min, T_R=25°C, T_H=40°C, t_s=24 min.

4.3.2 Experimental results and comparison with EDM predictions

Single component wide pulse injections were performed to validate adsorption behaviour in segmented gradient according to the switch time, as mentioned in Fig. 1.

When the switch is at t=0, as shown in Fig. 6(a) corresponding to Fig. 1(a), the Segment 1 was placed in the HPLC oven and maintained at 25 °C whereas the Segment 2 was placed in the water jacket and its temperature was maintained by thermostats at T_R=25°C, T_L=10 °C and T_H=40 °C, respectively. As a result, the plateaus were just shifted in retention time while keeping their width and height unchanged due to the fact the front and tail underwent the same temperature change at the same position.

In the experimental gradient operation with full modulation, as shown in Fig. 6(b), the temperatures in both columns were initially maintained at 25 °C before being changed manually in Segment 2 at a certain switch time t_s to T_R=25°C, T_L=10°C and T_H=40°C, respectively.

Since only Segment 2 is placed in the temperature modulating unit, the switch time should be after the desorption tail enters the Segment 2. If the switch time is too early, the profile behaves the same as Fig. 6(a), while if too late after desorption tail leaves the column, it becomes the mere isothermal case. The switch time was then set at t_s=18 min when both front and tail of the component were located in Segment 2 before leaving, corresponding to Fig. 1(b). As a consequence, the width and height of the plateau were changed. It is due to the fact that the front and tail were simultaneously influenced by temperature, thereby changing the width and height accordingly while keeping constant area, to meet mass balance.

The gradient operation with partial modulation, corresponding to Fig. 1(c) was also illustrated, as shown in Fig. 6(c). The switch time was set at t_s=24 min when the front leaves the column whereas the tail is still inside the column, i.e., the component is at the halfway of leaving the column when the front already appeared on the detector at 22 min. Upon switching to higher or lower temperature, the profile appeared in a splitting manner due to the fact that the tail inside column underwent the temperature change thereby varying width and height while keeping constant area.

In all cases, numerical solutions using EDM with $\overline{N_p}$=2871 (Table 2, Eq. (12)) are compared with actual experimental profiles. It can be seen that both profiles relatively showed a good agreement since the numerical solution captured correct trends towards temperature modulation. However, small difference still existed. Such differences can be attributed to several aspects. First, errors from Henry constants might exist. The actual temperatures of both segments might not be perfectly consistent since the temperature controlling media were different and the Henry constants were determined based on water jacket temperature. Second, temperature uncertainties caused by the operation of the thermostat exist. For example, during the switch from cold water (Thermostat 1) to hot water (Thermostat 2), the hot water temperature in Thermostat 2 is not kept constant. Although the thermostat is soon restoring the setting temperature, a delay was unavoidable. This kind of temporal temperature change cannot be ignored especially in the cooling operation since it is more difficult than heating. Additionally, a dead time for the water exchange in the water jacket also exists, which was difficult to measure. Third, the ideal step gradient was used in the model. However, the actual temperature profile should not be step-like, but rather curved, i.e., a smoothened step gradient. In real experiments, the column requires time to approach a

specified temperature upon switching and cannot reach that exact value due to heat transfer resistance. Last, thermal dispersion was neglected in the model, i.e., model limitation. Both axial and radial thermal dispersion might play important roles for the elution profiles. A more detailed 2D model is under development.

4.4 Separation of the ternary model mixture using temperature gradients

In the mixture experiments, the aforementioned temperature gradient operations were performed aiming at reducing cycle time thereby solving partly lagged separation problems. The flow rate was set as 0.3 mL/min and the dead time was determined to be 0.25 min. The injection volume was set as 400 µL, which was determined by finding maximal loadability while getting perfect baseline separation for all components at reference temperature 25 °C. Gradients can be applied according to certain strategies. In the current work, a conservative scheme and improved scheme are presented. The analytical solutions using the EM and numerical solutions using EDM were also provided for comparison with experiment. The switch times were determined by calculation of start and end positions in simulation study whereas by observation in experimental implementation. The switch time from high temperature T_L to low temperature T_H in kth cycle is notated as t_{s1}^k, whereas that from low temperature to high temperature as t_{s2}^k. These characteristic switch times are the key information for the repetitive batch chromatography. To deliver it in a simple way, switch times can be expressed by the switch times relative to the start time of injection in the same repetitive cycle:

$$\Delta t_{s1} = t_{s1}^k - t_{inj}^k \tag{17}$$

$$\Delta t_{s2} = t_{s2}^k - t_{inj}^k \tag{18}$$

It should be noted that kth cycle should be counted from the repetitive cycle since the first cycle might be different from others in some strategies.

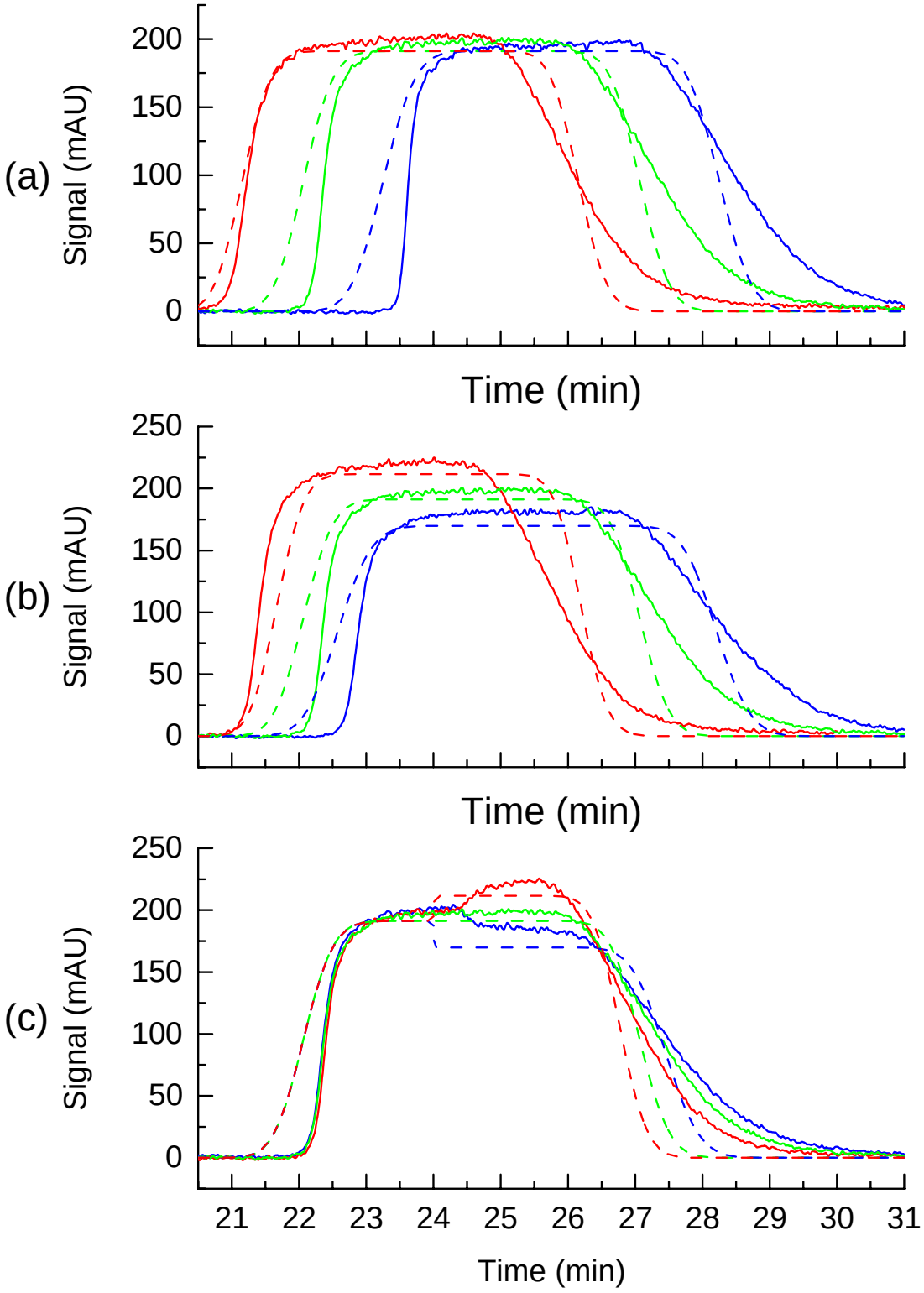

Fig. 6. Single component wide pulse experiment according to different switch time. Solid line represents experimental profile and dashed line numerical solution using the EDM with $\overline{N_p}$=2871. The green line corresponds to isothermal operation at T_R=25°C while the red and blue lines are for gradient operation by heating T_H=40°C and cooling T_L=10°C on the Segment 2, respectively. (a) t_s=0, corresponding to Fig. 1(top); (b) t_s=18 min, corresponding to Fig. 1(middle); (c) t_s=24 min, corresponding to Fig. 1(c) and Fig. 5. $c_{f,C7}$ =0.956 g/L, V_{inj}=1500 µL, t_d=3.246 min, $\dot{V}$=0.3 ml/min.

4.4.1 Conservative scheme with safety margins

According to the analytical study, gradient deployment was subjected to the principal strategy that fast components should be cooled to decelerate and slow components should be heated to accelerate. However, due to the segment nature, the temperature modulating unit cannot simultaneously perform heating and cooling. Under a safety margin, the switch from heating to cooling should be done after the last eluting component completely leaves the column, as shown in Fig. 7. Thus, the first eluting component in the new cycle should just reach Segment 2 while the last eluting component in previous cycle just leaves the Segment 1, which leads to a delay of start time of the new injection. As a consequence, a second safety time Δt_{safe}^{Temp} is relevant which accounts for this delay caused by non-ideal implementation of temperature:

$$\Delta t_{safe}^{Temp} = t_{1,start}^{k}\Big|_{c_{thres}} - t_{N,end}^{k-1}\Big|_{c_{thres}} \tag{19}$$

This safety time is reflected as a gap between consecutive injections in the chromatogram and differs in theoretical models and experiments. Based on this principle, the periodic switch times and injection times can be calculated in the analytical and numerical solutions. In the experiment, the switch times can be directly determined from the chromatogram whereas injection timings can be determined by subtracting the residence time of the front point in a single column at reference temperature from the end point in the foregoing cycle. In experiment the start time for the second injection was determined to be 15.5 min. The cycle time was determined to be 11.4 min. However, a gap between the consecutive injections was generated. As a result, by applying such a scheme the cycle time was even longer than the isothermal operation. Hence, this kind of gradient scheme is rather conservative but not optimal. Additionally, the numerical solution met good agreement with that in the analytical solution. It is noticed that there is a shift for the second cycle in the numerical solution since the dispersion effect is taken into account in the determination of the start time of injections, the switch times (Eq. (17)-(18)) and also the safety times (Eq. (19)). They directly influence the cycle time. The safety margin of EDM was determined to be 1.3 min. The numerical solution was also compared with the experimental profile, as shown in Fig. 8. It can be seen that the numerical solution fits the experimental profile quite well. The shift between the elution profiles in the second cycle is due to different criteria for cycle time determination in simulation and experiment. The real temperature profile (right axis) is not the projected perfect step-gradient, but characterised rather by a transition with a slow final asymptote.

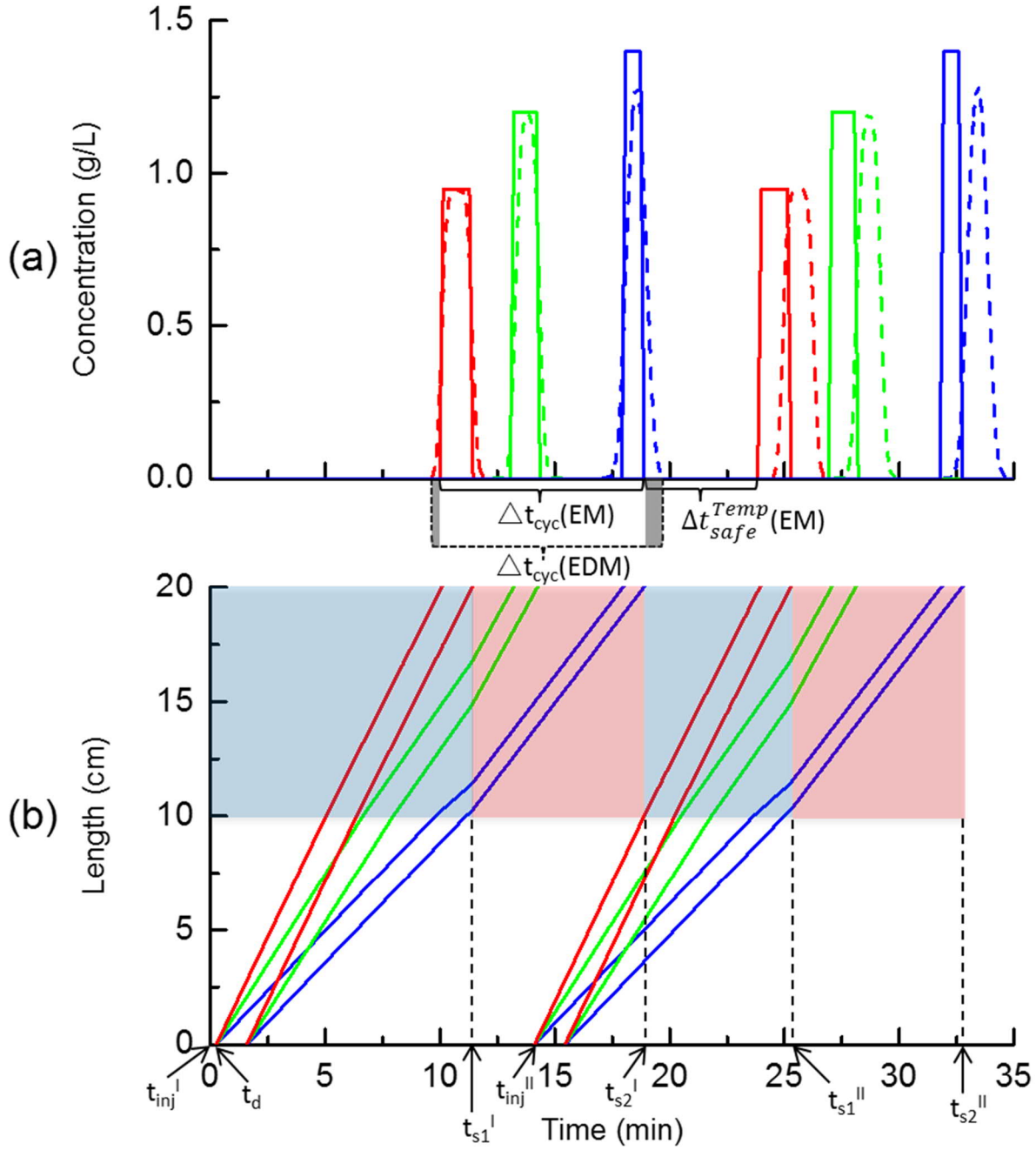

Fig. 7. Predicted chromatograms at z=L for temperature gradient operation. The red, green and blue lines correspond to C5, C6 and C7, respectively. (a) Analytical solution using EM (solid) and numerical solution using EDM (dashed). (b) Trajectory plot from analytical solution. The blue and red blocks indicate theoretical cooling at T_L=5°C and heating at T_H=60°C operation whereas the white block reference temperature at T_R=25°C. The grey area indicates the extra safety time for model compensation Δt_{safe}^{Mod} according to Eq. (16). Furthermore, an extra safety time Δt_{safe}^{Temp} (Eq. (19)) accounts for the non-ideal implementation of the temperature gradient, just shown for EM in the figure. $c_{f,C5}$=0.949 g/L, $c_{f,C6}$=0.948 g/L, c_{thres}=10^{-3} g/L, $c_{f,C7}$=0.956g/L, V_{inj}=400 µL, t_d=0.25 min, $\dot{V}$ =0.3 ml/min, $\overline{N_p}$ =2871. t_{inj}^{II}(EM)=13.9min, t_{s1}^{I}(EM)=11.2 min, t_{s2}^{I}(EM)=18.6 min, t_{s1}^{II}(EM)=25.0 min, t_{s2}^{II}(EM)=32.7 min, Δt_{cyc}(EM)=8.8 min, Δt_{safe}^{Temp}(EM)=5.2 min.

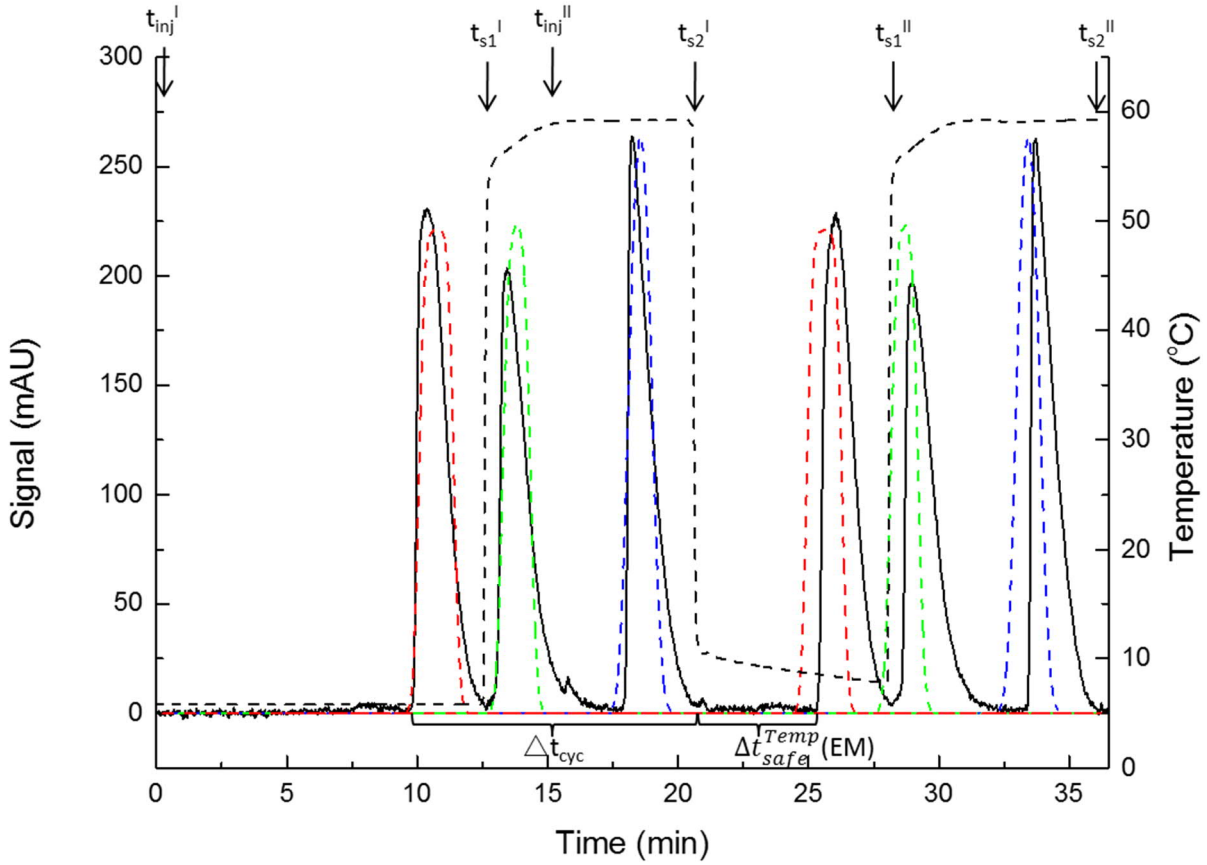

Fig. 8. Comparison between numerical solution (coloured dashed lines) and experimental component profile (solid lines) with temperature profile (black dashed, right axis) under gradient operation by conservative scheme. The red, green and blue lines correspond to C5, C6 and C7, respectively. $c_{f,C5}$=0.949 g/L, $c_{f,C6}$=0.948 g/L, $c_{f,C7}$=0.956g/L, c_{thres}=10^{-3} g/L, V_{inj}=400 µL, t_d=0.25 min, $\dot{V}$ =0.3 ml/min, $\overline{N_p}$ =2871. t_{inj}^{II}(EDM)= 15.0 min, t_{s1}^{I}(EDM)=11.6 min, t_{s2}^{I}(EDM)=19.5 min, t_{s1}^{II}(EDM)=26.6 min, t_{s1}^{II}(EDM)=34.8 min, Δt_{cyc}(EDM)=10.1 min, Δt_{safe}^{Mod}=1.3 min, Δt_{safe}^{Temp}(EDM)=4.9 min, t_{inj}^{II}(EXP)=15.5 min, t_{s1}^{I}(EXP)=12.5 min, t_{s2}^{I}(EXP)=20.5 min, t_{s1}^{II}(EXP)=28.0 min, t_{s2}^{II}(EXP)=35.8 min, Δt_{cyc}(EXP)=11.4 min, Δt_{safe}^{Temp}(EXP)=4.1 min.

4.4.2 Potential for improving productivity

The above gradient operation can be improved by reducing or even completely eliminating the safety time for non-ideal implementation of temperature gradient, Δt_{safe}^{Temp} (Eq. (19)). Namely, the start time of the new injection can be adjusted to make the chromatograms fully connected without any gaps, as shown Fig. 9. As a result, the first eluting component in the new cycle undergoes a complicated temperature regime. The front is heated together with the last eluting component from the previous cycle whereas the tail is partially cooled after the front reaches the outlet. This subsequent cooling for the first eluting component is not

aimed at cycle time reduction, but at maintaining the resolution. Without this cooling process the first and second eluting components were remixed again. The contribution of cycle time reduction is then attributed to heating of the last eluting components. Based on this strategy, the start time of injection and switch times were adjusted in simulations. In the experiment, the start time of injection can be determined by the difference between the end point of the last eluting component and the start point of the first eluting component that can be measured from a simple T_R-T_H gradient operation. The determination was based on experimental observation from the chromatograms and empirical tuning. Consequently, the start time for the second injection was determined to be 9.5 min in EM, 11 min in EDM and 11.5 min in the experiment. Remarkably, the cycle time for first cycle should be different compared to others due to different temperature conditions, which is reflected in the height difference between the first and second cycles. The first cycle was same as that in the conservative scheme since their temperature conditions were identical. The cycle time from the second cycle was determined to be 9.6 min in EM, 10.5 min in EDM and 11.1 min in the experiment. The cycle time was smaller than that for isothermal operation, which manifests an improved productivity. Similar to the conservative scheme, the cycle time of numerical solution was longer than that of the analytical solution due to dispersion. The numerical solution was in good agreement with the experimental profile, shown in Fig. 10. The small shift of the second cycle is attributed to the different criteria for cycle time determination.

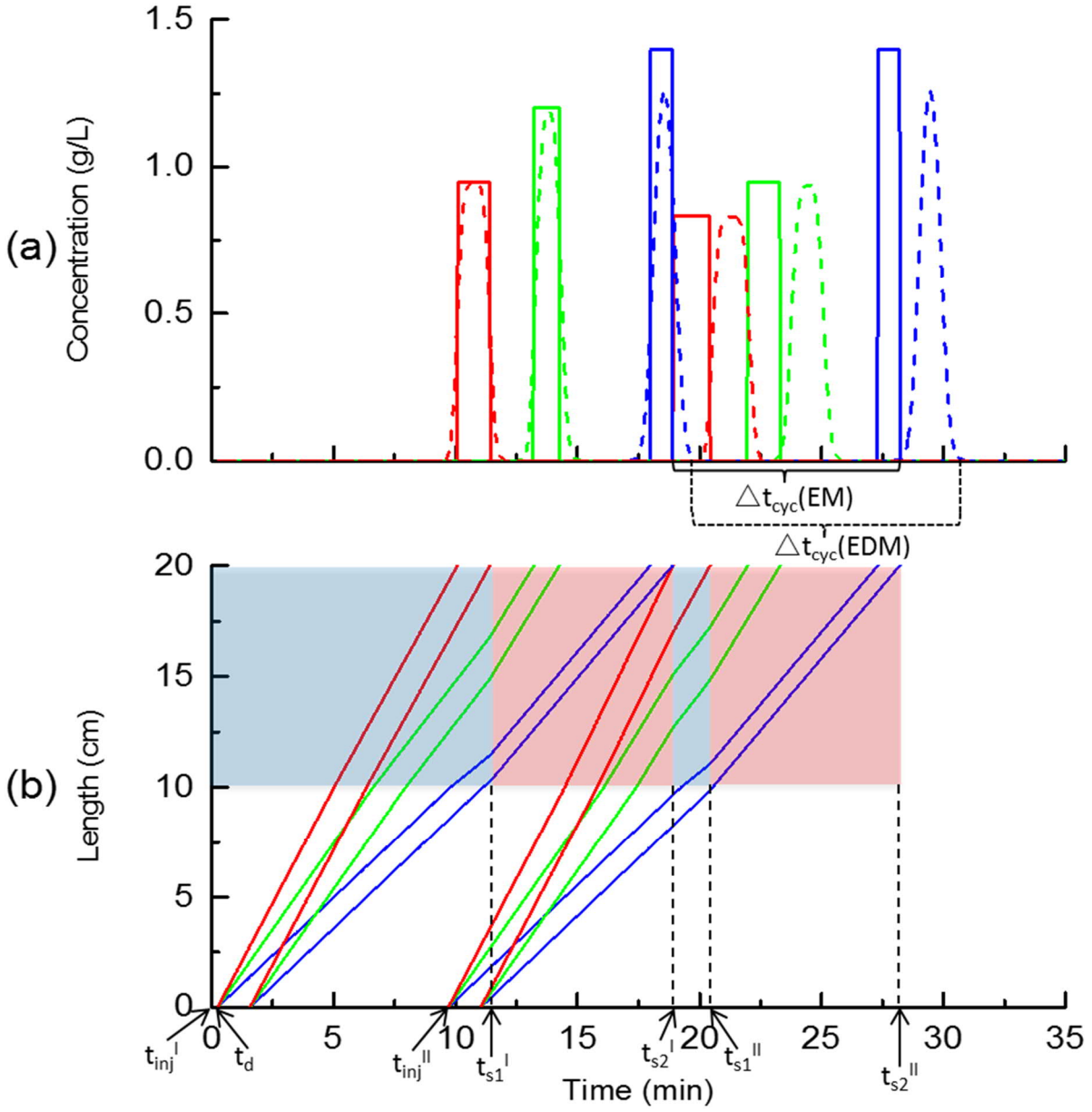

Fig. 9. Predicted Chromatograms at z=L under gradient operation by improved scheme. The red, green and blue lines correspond to C5, C6 and C7, respectively. (a) Analytical solution using EM (solid) and numerical solution using EDM (dashed). (b) Trajectory plot from analytical solution. The blue and red blocks indicate theoretical cooling at T_L=5°C and heating at T_H=60°C operation whereas the white block reference temperature at T_R=25°C. $c_{f,C5}$=0.949 g/L, $c_{f,C6}$=0.948 g/L, $c_{f,C7}$=0.956g/L, c_{thres}=10^{-3} g/L, V_{inj}=400 µL, t_d=0.25 min, $\dot{V}$=0.3 ml/min, $\overline{N_p}$=2871. t_{inj}^{II}(EM)= 9.5min, t_{s1}^{I}(EM)=11.2min, t_{s2}^{I}(EM)=18.6min, t_{s1}^{II}(EM)=20.2min, t_{s1}^{II}(EM)=28.2min, Δt_{cyc}(EM)=9.6min, Δt_{safe}^{Temp}(EM)=0 min.

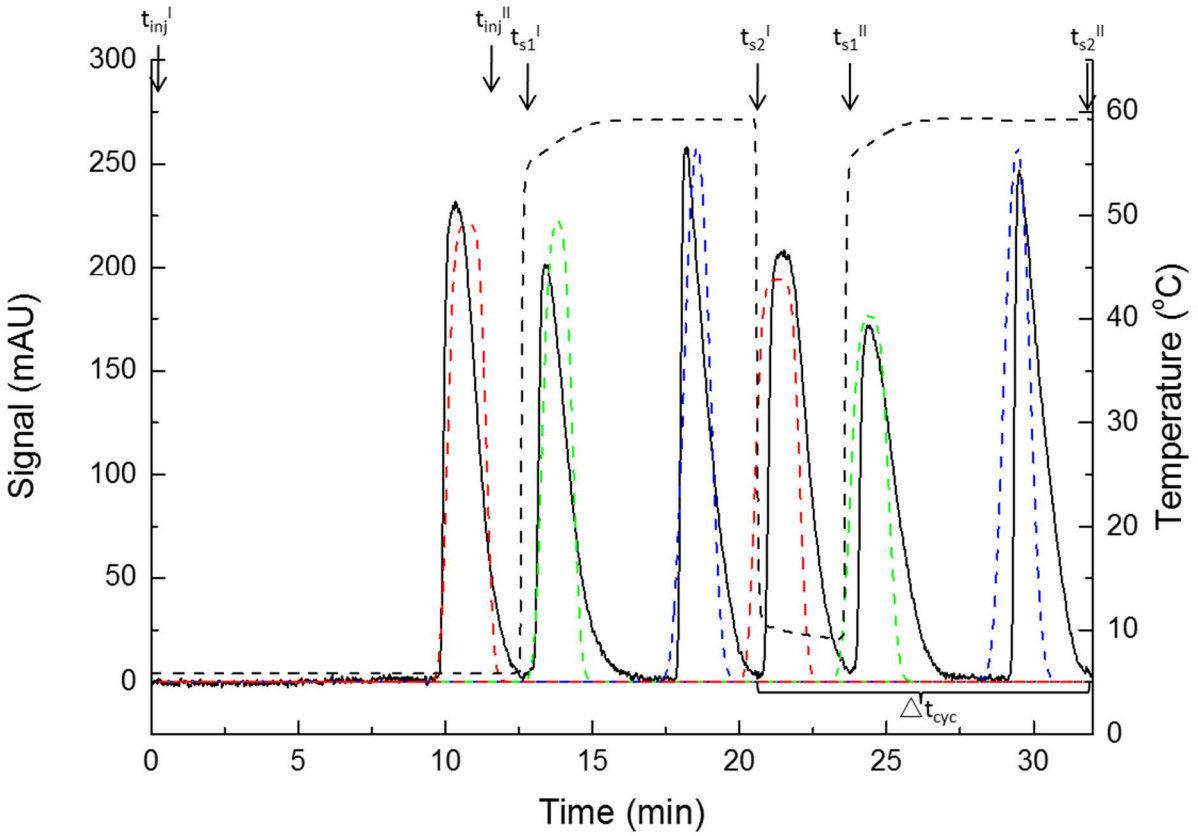

Fig. 10. Comparison between numerical solution (colour dashed) and experimental component profile (solid) with temperature profile (black dashed, right axis) under gradient operation by improved scheme. The red, green and blue lines correspond to C5, C6 and C7, respectively. $c_{f,C5}$=0.949 g/L, $c_{f,C6}$=0.948 g/L, $c_{f,C7}$=0.956g/L, c_{thres}=10^{-3} g/L, V_{inj}=400 µL, t_d=0.25 min, $\dot{V}$ =0.3 ml/min, $\overline{N_p}$ =2871. t_{inj}^{II}(EDM)=11.0min, t_{s1}^{I}(EDM)=11.6min, t_{s2}^{I}(EDM)=19.5min, t_{s1}^{II}(EDM)=21.2min, t_{s2}^{II}(EDM)=30.6min, Δt_{cyc}(EDM)=10.5min, Δt_{safe}^{Mod} =0.9 min, Δt_{safe}^{Temp} (EDM)=0 min, t_{inj}^{II}(EXP)=11.5min, t_{s1}^{I}(EXP)=12.5min, t_{s2}^{I}(EXP)=20.5min, t_{s1}^{II}(EXP)=23.5min, t_{s2}^{II}(EXP)=32.0min, Δt_{cyc}(EXP)=11.1min, Δt_{safe}^{Temp}(EXP)=0 min.

4.4.3 Reduction of productivity due to dispersion

It is noticed that the productivity or cycle time is also influenced by dispersion, or theoretical plate number as in Eq. (11) since less dispersion means shorter cycle time and larger productivity. Hence, the effect of theoretical plate number on productivity of the target component and cycle time applying the improved gradient scheme was simulated for confirmation, as shown in Fig. 11. It can be seen from the figure that the productivity increased significantly when the plate number was less than 2000 and after that tended to approach a maximum productivity of 0.713 g.hr^{-1}L^{-1} corresponding to a minimum cycle time of 9.6 min where the equilibrium model was applied, i.e. $\overline{N_p} = \infty, \overline{D_{app}} = 0$. Hence, the suggested

theoretical plate number was observed to be above 2000 at a flow rate of 0.3 ml/min in order to increase the productivity under current operation conditions. As aforementioned, the safety time is needed for model compensation with respect to EM, corresponding to black arrows in the figure. It can be also seen that as safety time increases, cycle time increases and productivity decreases. To compensate the deficits of EM in a conservative manner, the suggested safety time is ca. 25% of the cycle time calculated by EM. Notably, the cycle time of the numerical solution with infinite plate number using EDM is bigger than that of analytical solution using EM due to unavoidable numerical dispersion.

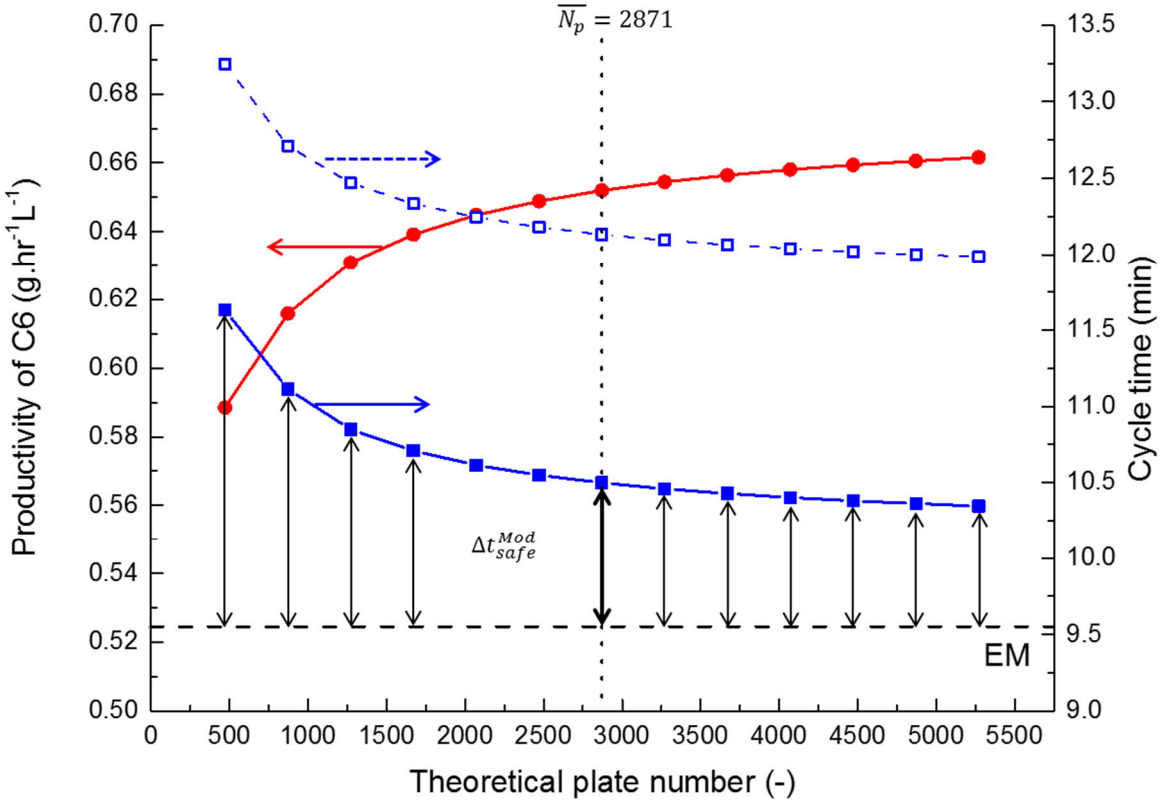

Fig. 11. Effect of theoretical plate number on productivity (left axis) and cycle time (right axis) by improved scheme. Δt_{safe}^{Temp}(EDM) is assumed to be zero (Eq. (19)). The empty symbols with dashed line represents the case of isothermal operation at 25 °C. $c_{f,C5}$=0.949 g/L, $c_{f,C6}$=0.948 g/L, $c_{f,C7}$=0.956g/L, , c_{thres}=10^{-3} g/L, V_{inj}=400 µL, t_d=0.25 min, $\dot{V}$=0.3 ml/min, T_L=5°C, T_H=60°C.

4.4.4 Repetitive batch injections

Four consecutive injections were carried out applying the improved injection scheme without the safety time in order to verify the reproducibility and stability. The results are shown in Fig. 12. On the right axis, the measured water temperature T^A is shown as a dashed line, and the corresponding outlet temperature T^B is given as a dotted line. The thermostats have a transition behaviour in water exchange from the water jacket upon switching so that the water temperature cannot change perfectly as planned. It can be seen that profiles from the second cycle were in a repeatable manner so that temperature gradient operation was confirmed to be reproducible and stable. All characteristic times including start times of injection t_{inj}^k, switch times t_{s1}^k, t_{s2}^k as well as relative switch times Δt_{s1}, Δt_{s2} are marked in the figure. The isothermal operation was also carried out for comparison. The start times of injections under the gradient operation were earlier than those under the isothermal operation, which is attributed to the reduction of the cycle time. Additionally, there was a little difference between both operations in the start point of elution bands since their temperature conditions were different, however, it was very small due to the low thermal sensitivity of the first eluting component.

The cycle times, productivities, start times for the second injection, switch times, relative switch times and safety times for different scenarios in theories and experiments are summarised in Table 4. The cycle time under the isothermal operation as reference was 12.7 min and a reduction up to 11.1 min could be achieved under the gradient operation (a decrease of 12.6%). The corresponding productivity was increased by approx. 14.5%. The cycle time using EDM was longer than that using EM due to the fact that the dispersion increases the cycle time. However, it was shorter than that in the experiment since the non-ideal tailing phenomena exists in the real process. The relative switch times, Δt_{s1} and Δt_{s2} (Eq. (17)-(18)), for the system studied were determined to be 12.0 min and 20.5 min, respectively. The safety times for compensating model errors (Eq. (16)) in conservative and improved schemes were determined to be 1.3 min and 0.9 min, respectively. They were quite small so that that the EDM was turned out to be reliable and useful for fast prediction. Another safety time for non-implementation of temperature gradient depends on operation strategies, which can be remained or eliminated. However, it should in principle ensure no remixing for the target component. In this study, all components were designed to be fully separated. In case of

centre-cut separations, one can also allow the remixing of the first and the last eluting components between cycles in order to further increase the productivity of the target component.

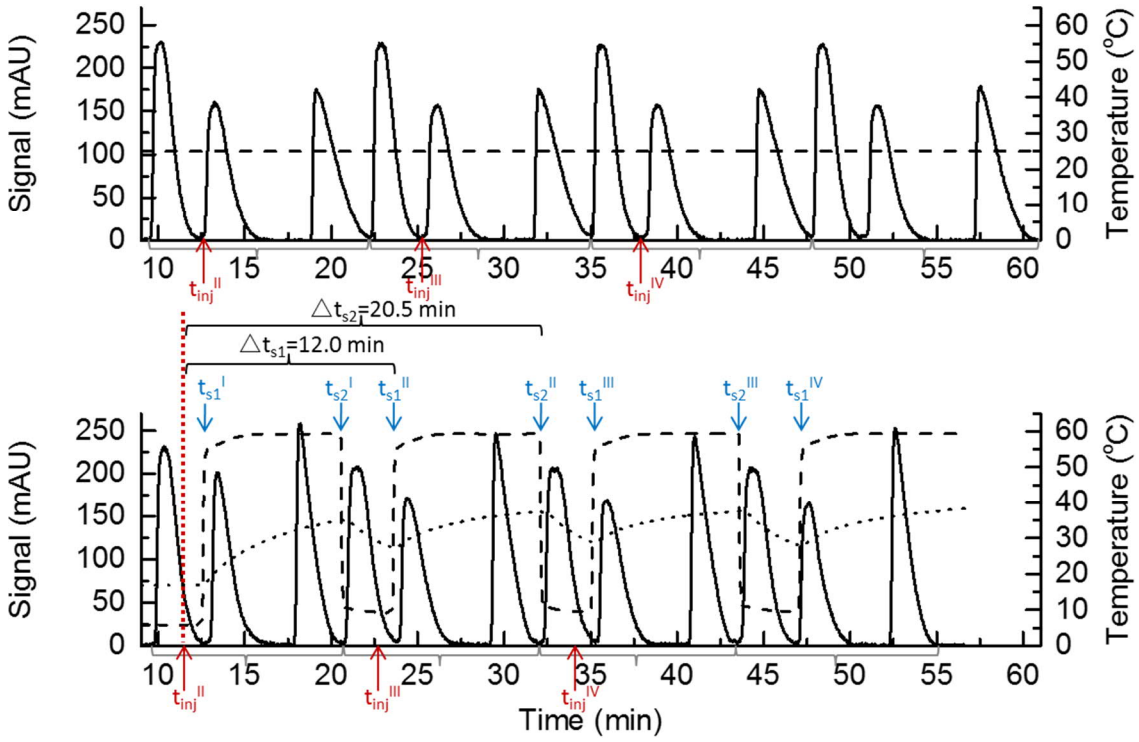

Fig. 12. Comparison of (top) isothermal operation at T_R=25°C, (bottom) gradient operation with improved scheme. T_L=5°C, T_H=60°C. The solid line corresponds to chromatogram (left axis), dashed line to measured water temperature T^A, dotted line to measured outlet temperature T^B (right axis). $c_{f,C5}$=0.949 g/L, $c_{f,C6}$=0.948 g/L, $c_{f,C7}$=0.956g/L, V_{inj}=400 µL, t_d=0.25 min, $\dot{V}$=0.3 ml/min. Top: Δt_{cyc}=12.7 min, Bottom: Δt_{cyc}=11.1 min, Δt_{s1}=12.0 min (Eq. (17)), Δt_{s2}=20.5 min (Eq. (18)).

Table 4 Summary of cycle times (Δt_{cyc}), productivity (P) and switch times (t_s) in different scenarios (t_{inj}^{I}=0 min).

Operation mode		Δt_{cyc} (min) Eq. (15)	$P_{i=C6}$ (g.hr^{-1}L^{-1}) Eq. (14)	t_{inj}^{II} (min)	t_{s1}^{I} (min)	t_{s2}^{I} (min)	t_{s1}^{II} (min)	t_{s2}^{II} (min) Pattern continued: t_{s1}^{III}...	Δt_{s1} (min) Eq. (17)	Δt_{s2} (min) Eq. (18)	Δt_{safe}^{Mod} (min) Eq. (16)	Δt_{safe}^{Temp} (min) Eq. (19)	Figure
Isothermal (25°C)	EXP	12.7	0.539	12.7	-	-	-	-	-	-	-	-	Fig. 12(a)
Conservative: T_L=5°C,T_H=60°C	EM	8.8	0.489	13.9	11.2	18.6	25.0	32.7	11.1	18.8	-	5.2	Fig. 7-Fig. 8
	EDM*	10.1	0.456	15.0	11.6	19.5	26.6	34.8	11.6	19.8	1.3	4.9	
	EXP	11.4	0.442	15.5	12.5	20.5	28.0	35.8	12.5	20.3	-	4.1	
Improved: T_L=5°C,T_H=60°C	EM	9.6	0.713	9.5	11.2	18.6	20.2	28.2	10.7	18.7	-	0.0	Fig. 9-Fig. 10, Fig. 12(b)
	EDM*	10.5	0.652	11.0	11.6	19.5	21.2	30.6	10.2	19.6	0.9	0.0	
	EXP	11.1	0.617	11.5	12.5	20.5	23.5	32.0	12.0	20.5	-	0.0	

EM: Equilibrium model, EDM: Equilibrium-dispersion model, EXP: Experiment.

* $\overline{N_p}$=2871 ($\overline{D_{app}}$=0.0057 cm^2/min), c_{thres}=10^{-3} g/L in Eq. (15).

5. Conclusions

Theoretical and experimental investigations of forced segmented temperature gradient for liquid chromatography were carried out. The effects of temperature gradients on the retention behaviours were verified and the separation performances in terms of cycle time and productivity were evaluated. For simplicity, the step gradient was applied in both theoretical and experimental studies. The key features of temperature gradients were experimentally demonstrated by the elution profiles of single component wide pulse injections. Both the analytical solutions using EM and the numerical solution using EDM can qualitatively predict the retention behaviours in a consistent manner. It was also confirmed that the dispersion effect can lead increase in the cycle time and decrease in productivity. The separation of a ternary model mixture aiming at cycle time reduction under repetitive injections applying temperature gradient was carried out. Suitable process parameters, especially switch times for temperature switches were identified to minimise the cycle time thereby increasing the productivity. Compared to the isothermal operation, the productivity of the target component applying the described temperature gradient was increased. The possibilities of segments in different length have not been discussed here. The model deficits of EM were evaluated in terms of safety time. A second safety time could be deployed for the non-ideal implementation of temperature gradient. In order to describe the temperature step gradient more precisely and to account for non-ideality of the step gradient, a more detailed two-dimensional model including the real implemented temperature profiles will be studied in future work.

Acknowledgment

This work was supported by Max Planck Society and International Max Planck Research School.

References

[1] G. Guiochon, A. Felinger, D.G.G. Shirazi, A.M. Katti, Fundamentals of Preparative and Nonlinear Chromatography, 2nd ed., Academic Press, Boston, MA, 2006.

[2] H. Schmidt-Traub, M. Schulte, A. Seidel-Morgenstern, Preparative Chromatography: Second Edition, 2013. https://doi.org/10.1002/9783527649280.

[3] D.B. Broughton, C.G. Gerhold, Continuous sorption process employing fixed bed of sorbent and moving inlets and outlets, (1961) US Patent 2 985 589.

[4] A. Rajendran, G. Paredes, M. Mazzotti, Simulated moving bed chromatography for the separation of enantiomers, J. Chromatogr. A. 1216 (2009) 709–738. https://doi.org/10.1016/j.chroma.2008.10.075.

[5] P. Jandera, J. Churáček, Gradient elution in column liquid chromatography : theory and practice, J. Chromatogr. Libr. 31 (1985) 1–510.

[6] L. Aumann, M. Morbidelli, A Continuous Multicolumn Countercurrent Solvent Gradient Purification (MCSGP) Process, Biotechnol. Bioeng. 98 (2007) 1043–1055. https://doi.org/10.1002/bit.

[7] A. Damtew, B. Sreedhar, A. Seidel-Morgenstern, Evaluation of the potential of nonlinear gradients for separating a ternary mixture, J. Chromatogr. A. 1216 (2009) 5355–5364. https://doi.org/10.1016/j.chroma.2009.05.026.

[8] G. Carta, W.B. Stringfield, Analytic solution for volume-overloaded gradient elution chromatography, J. Chromatogr. A. 605 (1992) 151–159. https://doi.org/10.1016/0021-9673(92)85232-I.

[9] B. Sreedhar, A. Seidel-Morgenstern, Preparative separation of multi-component mixtures using stationary phase gradients, J. Chromatogr. A. 1215 (2008) 133–144. https://doi.org/10.1016/j.chroma.2008.11.003.

[10] L.N. Jeong, S.C. Rutan, Simulation of Elution Profiles in Liquid Chromatography - III. Stationary Phase Gradients, J. Chromatogr. A. submitted (2018) 128–136. https://doi.org/10.1016/j.chroma.2018.06.007.

[11] G. Carta, A. Jungbauer, Protein Chromatography: Process Development and Scale-Up,

Wiley-VCH, 2010. https://doi.org/10.1002/9783527630158.

[12] C.A. Martínez Cristancho, A. Seidel-Morgenstern, Purification of single-chain antibody fragments exploiting pH-gradients in simulated moving bed chromatography, J. Chromatogr. A. 1434 (2016) 29–38. https://doi.org/10.1016/j.chroma.2016.01.001.

[13] T.M. Pabst, D. Antos, G. Carta, N. Ramasubramanyan, A.K. Hunter, Protein separations with induced pH gradients using cation-exchange chromatographic columns containing weak acid groups, J. Chromatogr. A. 1181 (2008) 83–94. https://doi.org/10.1016/j.chroma.2007.12.054.

[14] T.J. Trinklein, D. V. Gough, C.G. Warren, G.S. Ochoa, R.E. Synovec, Dynamic pressure gradient modulation for comprehensive two-dimensional gas chromatography, J. Chromatogr. A. 1609 (2020) 1–9. https://doi.org/10.1016/j.chroma.2019.460488.

[15] R.S. Alm, R.J.P. Williams, A. Tiselius, Gradient elution analysis, Acta Chem. Scand. 6 (1952) 826–836. https://doi.org/10.1039/AN9527700905.

[16] D.C. Fenimore, Gradient temperature programming of short capillary columns, J. Chromatogr. A. 112 (1975) 219–227. https://doi.org/10.1016/S0021-9673(00)99955-2.

[17] S. Qamar, F.A. Sattar, I. Batool, A. Seidel-Morgenstern, Theoretical analysis of the influence of forced and inherent temperature fluctuations in an adiabatic chromatographic column, Chem. Eng. Sci. 161 (2017) 249–264. https://doi.org/10.1016/j.ces.2016.12.027.

[18] A. Brandt, G. Mann, W. Arlt, Temperature gradients in preparative high-performance liquid chromatography columns, J. Chromatogr. A. 769 (1997) 109–117. https://doi.org/10.1016/S0021-9673(97)00235-5.

[19] S. Qamar, N. Kiran, T. Anwar, S. Bibi, A. Seidel-Morgenstern, Theoretical Investigation of Thermal Effects in an Adiabatic Chromatographic Column Using a Lumped Kinetic Model Incorporating Heat Transfer Resistances, Ind. Eng. Chem. Res. 57 (2018) 2287–2297. https://doi.org/10.1021/acs.iecr.7b04555.

[20] J.W. Lee, P.C. Wankat, Thermal simulated moving bed concentrator, Chem. Eng. J. 166 (2011) 511–522. https://doi.org/10.1016/j.cej.2010.11.009.

[21] C. Migliorini, M. Wendlinger, M. Mazzotti, M. Morbidelli, Temperature gradient operation of a simulated moving bed unit, Ind. Eng. Chem. Res. 40 (2001) 2606–2617. https://doi.org/10.1021/ie000825h.

[22] X. Jiang, L. Zhu, B. Yu, Q. Su, J. Xu, W. Yu, Analyses of simulated moving bed with internal temperature gradients for binary separation of ketoprofen enantiomers using multi-objective optimization: Linear equilibria, J. Chromatogr. A. 1531 (2018) 131–142. https://doi.org/10.1016/j.chroma.2017.11.045.

[23] P. Cao, T.K.H. Müller, B. Ketterer, S. Ewert, E. Theodosiou, O.R.T. Thomas, M. Franzreb, Integrated system for temperature-controlled fast protein liquid chromatography . II . Optimized adsorbents and ' single column continuous operation ,' J. Chromatogr. A. 1403 (2015) 118–131. https://doi.org/10.1016/j.chroma.2015.05.039.

[24] R. De Pauw, M. Pursch, G. Desmet, Using the column wall itself as resistive heater for fast temperature gradients in liquid chromatography, J. Chromatogr. A. 1420 (2015) 129–134. https://doi.org/10.1016/j.chroma.2015.10.005.

[25] W. Jin, P.C. Wankat, Thermal operation of four-zone simulated moving beds, Ind. Eng. Chem. Res. 46 (2007) 7208–7220. https://doi.org/10.1021/ie070047u.

[26] K. Horváth, S. Horváth, D. Lukács, Effect of axial temperature gradient on chromatographic efficiency under adiabatic conditions, J. Chromatogr. A. 1483 (2017) 80–85. https://doi.org/10.1016/j.chroma.2016.12.063.

[27] S. Wiese, T. Teutenberg, T.C. Schmidt, A general strategy for performing temperature-programming in high performance liquid chromatography-Prediction of segmented temperature gradients, J. Chromatogr. A. 1218 (2011) 6898–6906. https://doi.org/10.1016/j.chroma.2011.08.022.

[28] S. Teramachi, H. Matsumoto, T. Kawai, Direction of temperature gradient for normal-phase temperature gradient interaction chromatography in polystyrene fractionation, J. Chromatogr. A. 1100 (2005) 40–44. https://doi.org/10.1016/j.chroma.2005.09.023.

[29] I.L. Skuland, T. Andersen, R. Trones, R.B. Eriksen, T. Greibrokk, Determination of polyethylene glycol in low-density polyethylene by large volume injection

temperature gradient packed capillary liquid chromatography, J. Chromatogr. A. 1011 (2003) 31–36. https://doi.org/10.1016/S0021-9673(03)01186-5.

[30] J. Leppert, P.J. Müller, M.D. Chopra, L.M. Blumberg, P. Boeker, Simulation of spatial thermal gradient gas chromatography, J. Chromatogr. A. 1620 (2020) 460985. https://doi.org/10.1016/j.chroma.2020.460985.

[31] J.A. Contreras, A. Wang, A.L. Rockwood, H.D. Tolley, M.L. Lee, Dynamic thermal gradient gas chromatography, J. Chromatogr. A. 1302 (2013) 143–151. https://doi.org/10.1016/j.chroma.2013.06.008.

[32] K. Kaczmarski, M. Chutkowski, Impact of changes in physicochemical parameters of the mobile phase along the column on the retention time in gradient liquid chromatography. Part A – Temperature gradient, J. Chromatogr. A. 1655 (2021) 462509. https://doi.org/10.1016/j.chroma.2021.462509.

[33] H.-K. Rhee, R. Aris, N.R. Amundson, On the Theory of Multicomponent Chromatography, Philos. Trans. R. Soc. London. Ser. A, Math. Phys. Sci. 267 (1970) 419–455. https://doi.org/10.1007/BF01018308.

[34] A. Hayat, X. An, S. Qamar, G. Warnecke, A. Seidel-Morgenstern, Theoretical analysis of forced segmented temperature gradients in liquid chromatography, Processes. 7 (2019) 1–19. https://doi.org/10.3390/pr7110846.

[35] R.J. LeVeque, Finite Volume Methods, in: Finite Vol. Methods Hyperbolic Probl., Cambridge University Press, 2002: pp. 64–86. https://doi.org/10.1017/CBO9780511791253.005.